Simultaneous adsorption of Hg^{2+}, Cd^{2+} and Cu^{2+} ions from aqueous solution with mesoporous silica/DZ and conditions optimise with experimental design: kinetic and isothermal studies

Samaneh Nazerdeylami ✉, *Rouholah Zare-Dorabei*

Research Laboratory of Spectrometry & Micro and Nano Extraction, Department of Chemistry, Iran University of Science and Technology, Tehran 16846-13114, Iran
✉ *E-mail: Zaredorabei@iust.ac.ir*

Published in Micro & Nano Letters; Received on 11th December 2018; Revised on 20th January 2019; Accepted on 12th March 2019

This study used dithizon (DZ) and mesoporous as a sorbent for simultaneous removal of heavy metal (mercury, cadmium and copper) ions from aqueous solution and real samples. Santa Barbara Amorphous synthesised and characterised by X-ray diffraction, Fourier-transform infrared spectroscopy and Brunauer–Emmett–Teller. Heavy metal ions measured by atomic absorption spectrometry and inductively coupled plasma optical emission spectrometry. Optimised conditions such as pH, removal time, sorbent dosage and concentration analyte with central composite design and obtained 5, 20 min, 20 mg and 25 ppm, respectively. The equilibrium data were fitted to isotherm models such as Langmuir, Freundlich and Tempkin and the results revealed the suitability of the Langmuir model. The maximum adsorption capacities for Hg^{2+}, Cd^{2+} and Cu^{2+} ions achieved 25.04, 30.3 and 31.79 mg/g, respectively. Kinetics data fitting to pseudo-first order, pseudo-second-order and Elovich models confirmed the applicability of pseudo-second-order kinetic model for the description of the mechanism and adsorption rate. This sorbent could regenerate easily with ethylenediamminetetraacetate solution.

1. Introduction: Heavy metal ions are one of the world current problems; since, they are toxic pollutants, and have density more than 5 g/cm^3 and are widely applied in batteries, plastics, pigments, metal plating and petroleum [1–4]. The lawful amount of heavy metal ions such as Hg^{2+}, Cd^{2+} and Cu^{2+} in water according to World Health Organisation around 0.001, 0.003 and 2 mg/l, respectively [5].

High level of heavy metal ions especially cadmium, copper, mercury, silver and radioactive ions in aqueous solution are harmful to humans and ecosystems [6]. Such as mercury ion could pass skin, attracted central nervous system and effect on chromosomes [7, 8]. Cadmium ions could damage bones, lungs, livers, causing diarrhoea and metabolic disorders [9, 10]. Copper ions effect on eyes, bones, stomach and caused Menkes syndrome and Alzheimer's disease [11, 12]. Thus, we need that remove these pollutants. The several methods exist for removal such as reduction, coagulation, ion exchange, filtration and photocatalytic oxidation, electrodeposition, electrochemical, precipitation and membrane separation that among them adsorption is the best, rapid, easy and economical method [2, 13–15].

Several materials such as mesoporous silica, activated carbon, polymers, clays, talk, zeolite, fly ash and biomass are used for adsorption [16, 17]. Porous materials classified into three kinds by their pore size: macroporous (>50 nm), mesoporous (2–50 nm) and microporous (<2 nm). Mesoporous silica such as Santa Barbara Amorphous (SBA-15) with unique properties such as high specific surface area, good pore diameter (2–50 nm), highly nanoporous structures and thermally suitable for adsorption process [18–21].

Immobilisation of dithizon (DZ) in SBA-15 has been used to improve adsorption capacity and increase active sites because DZ as the ligand with –SH (thiol) and –NH (amin) groups was coupled with metal ions [17]. In this Letter, we simultaneously remove several ions from aqueous solution with SBA-15/DZ and optimised experimental conditions by central composite design (CCD). The adsorption isotherms and kinetics have also been investigated to display the adsorption mechanisms.

2. Materials and methods

2.1. Materials: All reagents and materials were used from Merck and Aldrich Co. $Hg(NO_3)_2$. H_2O, $Cd(NO_3)_2$. $4H_2O$ and $Cu(NO_3)_2$. $9H_2O$ salts from Merck Co. utilised for provided three stoke solutions (1000 ppm). Tetraethylorthosilicate (TEOS) and hydrochloric acid (HCl) solution from Merck Co. and Pluronic (P123, Mn = 5800, $EO_{20}PO_{70}EO_{20}$) from Aldrich Co. was used for synthesised SBA-15. DZ as a ligand utilised from Merck Co.

2.2. Apparatus: Analyte concentration was determined by inductively coupled plasma optical emission spectrometry (Shimadzu, ICPS-7000) and atomic absorption spectrometry (AAS) (Shimadzu, AA-6300). Fourier-transform infrared spectroscopy (FT-IR) (Shimadzu, 8400s), X-ray diffraction (XRD) (PANalytical, × Pert Pro MPD), Brunauer–Emmett–Teller (BET) (Micrometrics, ASAP-2020) were used for characterisation SBA-15.

2.3. Preparation of SBA-15: Mesoporous silica SBA-15 were synthesised by hydrothermal method [20, 22, 23]. About 4.00 g Pluronic (P123, Mn = 5800, $EO_{20}PO_{70}EO_{20}$), 90.0 ml of HCl 2.00 M and 21.00 ml deionised water were mixed at room temperature. In the next step, 6.40 g TEOS was added to the mixture and heated for 24 h at 40°c. Then, this blend was shredded in an autoclave at 100°C for 24 h. After these works, the gotten mixture was filtered and washed. The white powder was calcined at 600°C for 6 h.

2.4. Adsorption process: According to Fig. 1, first, heavy metal ions solution of Hg^{2+}, Cd^{2+} and Cu^{2+} with SBA-15 were shaked.

Second, 1.00 ml ethanolic solution consisting of DZ was added to the mixture and was shaked for a patch that formed $[M(DZ)_2]$ complex (Fig. 2). Then, the mixture was filtered and the solution below filter was analysed by ICP and AAS.

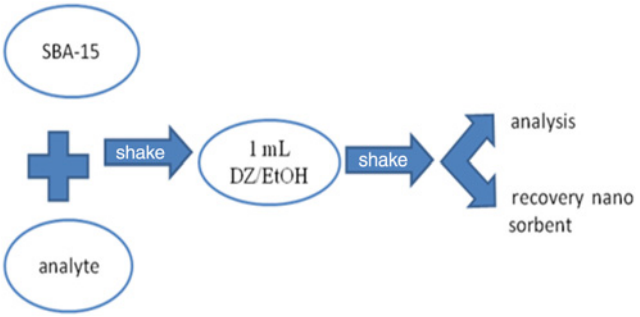

Fig. 1 *Adsorption process diagram*

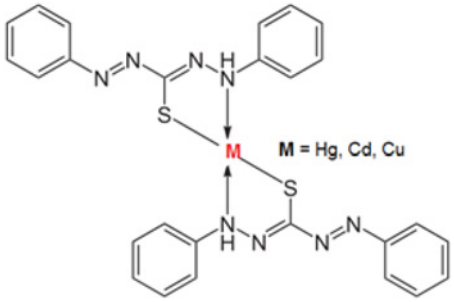

Fig. 2 *[M(DZ)$_2$] complex*

Table 1 Factors and their levels for the CCD

Factor	Symbols	Levels				
		$-\alpha$	−1	0	+1	$+\alpha$
pH	A	4.0	4.5	5.0	5.5	6.0
dose of adsorbent, mg	B	20.00	25.00	30.00	35.00	40.00
shaking time, min	C	20.00	22.50	25.00	27.50	30.00

Finally, adsorption capacity was calculated from the equation below:

$$q = \frac{V(C_o - C_t)}{M} \quad (1)$$

q is the adsorption capacity (mg/g); V is the volume of the solution (L); C_o is the initial concentration (mg/l); C_t is the equilibrium concentration (mg/l); and M is the amount of sorbent (g).

2.5. Design of experiments: The CCD was employed to investigate the effects of different operating factors on Cd(II), Hg(II) and Cu(II) adsorption capacity and reveal the optimum conditions for Cd(II), Hg(II) and Cu(II) removal as well as build models [24, 25]. By using the CCD method, 30 experiments (including six repetitions at a central point) were designed. The factors (variables) were: pH, a dose of adsorbent, shaking time and the ions concentration. For each factor, five levels were determined. These values are shown with $-\alpha$, −1, 0, +1 and $+\alpha$ codes in Table 1 ($\alpha = 2$).

3. Result and discussion

3.1. Characterisation: XRD pattern of the mesoporous silica SBA-15 and SBA-15/DZ is shown in Fig. 3. A strong peak (1 0 0) and two weak peaks (1 1 0) and (2 0 0) indicated that SBA-15 have hexagonal structure with symmetry P6mm. Constant peaks in SBA-15/DZ indicates modification of SBA-15 not affected in influence. Absorption of DZ caused decreases of intensity.

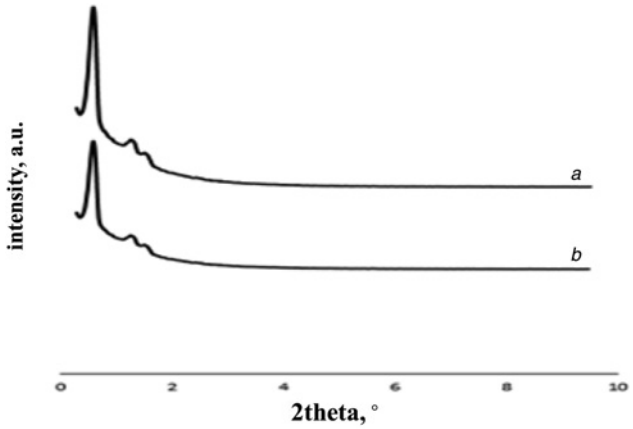

Fig. 3 *XRD pattern of the*
a SBA-15
b SBA-15/DZ

Here, $d_{1\ 0\ 0}$ achieved from XRD pattern was 9.05 nm. Then, the lattice parameter (a_0) was calculated and achieved 12.5 nm. The lattice parameter is estimated from the equation below:

$$a_0 = \frac{2d_{100}}{\sqrt{3}} \quad (2)$$

a_0 is the lattice parameter (nm) and $d_{1\ 0\ 0}$ is the distance of page (nm).

Fig. 4 shows BET analysis and sorption/desorption N_2 isotherm. BET analysis results were summarised in Table 2. Pore diameter and a wall thickness of mesoporous silica were achieved 85 A° (8.5 nm) and 4 nm, respectively. Absorption DZ on surface SBA-15 cased decreases total pore volume.

FT-IR spectrum results showed peaks in 3435, 1630, 1083 and 960 cm^{-1} corresponding to stretching vibration O–H bond in silanol group, vibration H_2O molecules that adsorption, vibration

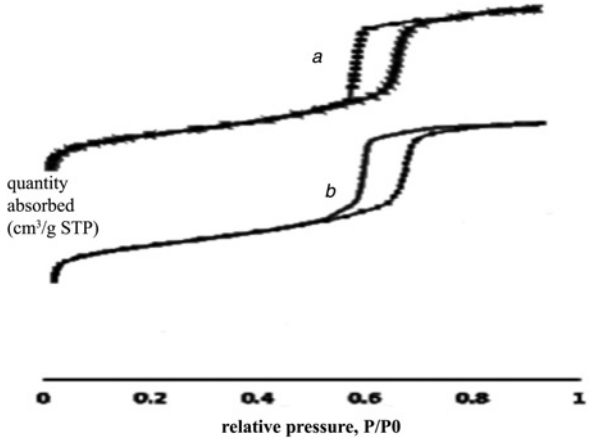

Fig. 4 *Sorption/desorption N_2*
a SBA-15
b SBA-15/DZ

Table 2 BET analysis of the SBA-15 and SBA-15/DZ

Sample	Surface area, m^2/g	Pore diameter (Barrett, Joyner and Halenda (BJH)), A°	Total pore volume, m^3/g
SBA-15	869	85	1.034
SBA-15/DZ	586	76	0.96

doi: 10.1049/mnl.2018.5775

Si–O–Si and Si–O bond in silanol group, respectively. Here, 1435 and 1532 cm^{-1} relative to C=S and C=N in SBA-15/DZ, respectively.

3.2. Modelling of adsorption: Experimental conditions are optimised by CCD. In the present work, the effects of four factors (pH, dosage adsorbent, removal time and initial heavy metal ions concentration) on sorption were studied.

The software package Design-Expert 7.0.0 was used to analyse the experimental data and to plot graphs. The correlation of removal of heavy metal ions and four experimental factors were got with coded variables below:

$$\begin{aligned}\text{adsorption capacity } Cd^{2+} = {} & 12.46 - 0.035A - 7.77B + 0.34C \\ & + 4.51D + 0.78AB - 0.034AC \\ & - 0.54AD + 0.16BC - 1.57BD + 0.13CD \\ & - 0.14A^2 + 3.85B^2 + 0.51C^2 + 0.12D^2\end{aligned} \tag{3}$$

$$\begin{aligned}\text{adsorption capacity } Hg^{2+} = {} & 12.43 + 0.83A - 4.75B + 0.11C \\ & + 4.11D - 0.35AB + 0.51AC \\ & + 0.26AD + 0.58BC - 1.4BD - 0.39CD \\ & - 0.51A^2 + 1.57B^2 - 0.086C^2 - 0.074D^2\end{aligned} \tag{4}$$

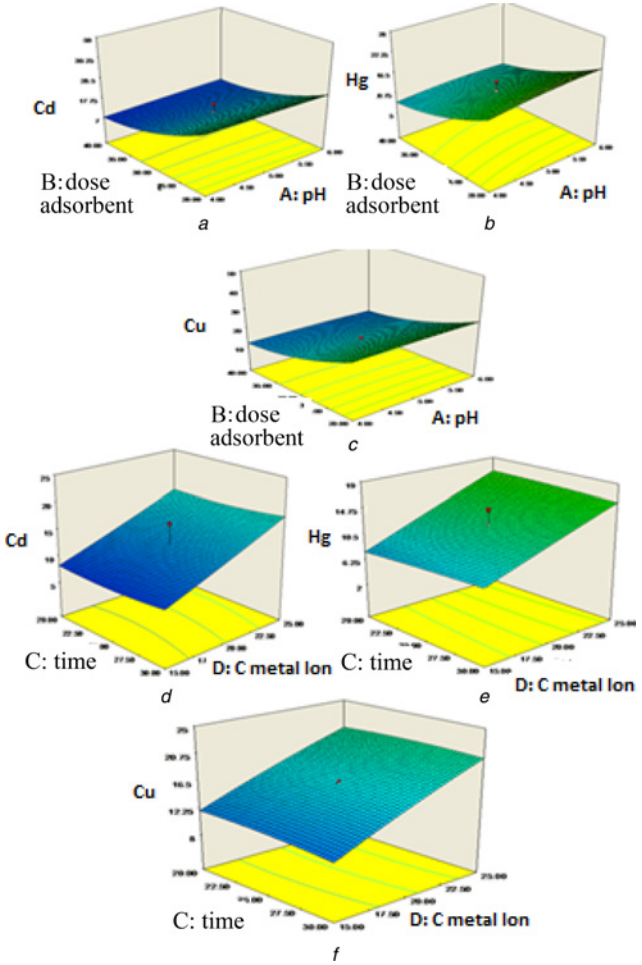

Fig. 5 *Effect of factors on sorption for*
a, *d* Cd^{2+}
b, *e* Hg^{2+}
c, *f* Cu^{2+}

$$\begin{aligned}\text{adsorption capacity } Cu^{2+} = {} & 16.67 - 0.18A - 7.43B - 0.18C \\ & + 4.44D - 0.2AB - 0.58AC \\ & + 0.2AD - 0.2BC - 0.98BD + 0.2CD \\ & - 0.31A^2 + 3.03B^2 - 0.31C^2 - 0.31D^2\end{aligned} \tag{5}$$

After studied analysis of variance for removal of Hg^{2+}, Cu^{2+} and Cd^{2+}, it is found that the quadratic model was good for these results. Lack of fit for three ions were low and not significant that indicated data were consented with the quadratic model. The coefficients of determination (R^2) for removal of Hg^{2+}, Cu^{2+} and Cd^{2+} were 0.97, 0.95 and 0.96, respectively.

3.3. Effect of factors, optimised conditions: Fig. 5 shows the effect of factors on sorption that time and pH have the lowest effect, unlike, adsorbent dosage and concentration analyte have the effect.

Finally, experimental conditions optimised for simultaneous adsorption of three heavy metal ions, where pH, removal time, dosage adsorbent and initial concentration equal 5.0, 20.00 min, 20.00 mg and 25.00 ppm, respectively.

3.4. Equilibrium isotherm models: The adsorption isotherm indicates how molecules of adsorbate are partitioned between the adsorbent and liquid phase at equilibrium as a function of adsorbate concentration [26, 27]. In this Letter, the equilibrium data obtained for the adsorptions of Hg^{2+}, Cu^{2+} and Cd^{2+} ions onto modified SBA-15 were analysed by considering the Langmuir, Freundlich and Tempkin isotherm model. R^2 values show that the Langmuir isotherm was good for adsorption of heavy metal ions.

Table 3 Parameters of adsorption isotherms

	Langmuir		Freundlich		Tempkin	
	Q_m, K_L	R^2	nK_F	R^2	B, K_T	R^2
Cu	21.739	1.1219	4.52	1.059	1.25	1.2
	0.999	—	0.832	—	0.941	—
Cd	18.181	1.1702	5.12	1.005	6.151	42.03
	0.999	—	0.834	—	0.847	—
Hg	23.809	1.0243	4.11	1.079	9.188	20.53
	0.921	—	0.998	—	0.899	—

Table 4 Parameters of the kinetic isotherm

	Pseudo-first order			Pseudo-second order		
	Q	K_1	R^2	Q_e	K_2	R^2
Cu	9.77	0.002	0.99	12.048	0.0246	0.998
Cd	12.317	0.001	0.998	13.333	0.0625	0.998
Hg	15.75	0.002	0.997	18.867	0.0173	0.999

Table 5 Report for adsorption of Hg^{2+}, Cu^{2+} and Cd^{2+} in real samples

Sample	Initial concentration, ppm			Added, ppm	Residual concentration, ppm		
	Hg^{2+}	Cu^{2+}	Cd^{2+}		Hg^{2+}	Cu^{2+}	Cd^{2+}
river water	0.00	0.00	0.00	25.00	3.63	2.45	1.74
shaft water	0.00	0.00	0.00	25.00	4.04	2.01	0.98
tap water	0.00	0.11	0.00	25.00	1.87	4.06	4.65

Table 6 Comparison of adsorption capacities Q_{max} (mg g^{-1}) of various adsorbents for heavy metal ions

Adsorbent	Q_{max}, mg g^{-1}			Contact time, min	References
	Hg	Cd	Cu		
montmorillonite–kaolinite/TiO_2 composite (simultaneous adsorption)	—	13.8	42.9	60	[28]
activated carbon cloth (simultaneous adsorption)	—	21.86	—	—	[29]
silica-3-chloropropyltriethoxysilane	48.14	—	—	—	[30]
silica-3-(2,2′-dipyridylamine) (DPA)	—	—	82.60	14	[31]
magnetic graphene oxide (GO) (simultaneous adsorption)	—	5.34	18.37	—	[32]
amino and thiolate-functionalised multiwall carbon nanotubes	85	—	—	60	[33]
GO-polydopamine	—	33.3	24.4	—	[34]
SBA-15/DZ	25.04	30.3	31.79	20	this work

The Langmuir (6) was explained by

$$q_e = \frac{C_e K_L Q_m}{1 + K_L C_e} \tag{6}$$

q_e is the equilibrium adsorption capacity (mg/g); C_e is the equilibrium concentration (mg/l); Q_m is the maximum adsorption capacity (mg/g); K_L is the Langmuir constant (l/mg); and Q_m and K_L obtained from the slope and intercept of the C_e/q_e versus C_e curve, respectively (Table 3).

3.5. Adsorption kinetics: A kinetic study of adsorption is necessary as it provides information about the adsorption mechanism, which is crucial for the practicality of the process. In this Letter, two different kinetic models were applied in order to establish which of them shows the best fit with experimentally obtained data.

R^2 values in Table 4 indicate that the adsorption process obeyed pseudo-second-order kinetic isotherm in the equation below:

$$\frac{t}{Q_t} = \frac{1}{K_2 Q_e^2} + \frac{t}{Q_e} \tag{7}$$

t is the time (min); K_2 is the pseudo-second-order constant (g/mg min); Q_e is the equilibrium adsorption capacity (mg/g); and Q_t is the adsorption capacity at any time (mg/g).

3.6. Adsorption of real samples and recovered: According to the results in Table 5, SBA/[$M(DZ)_2$] was good for treatment of real samples such as river water, shaft water and tap water. SBA/[$M(DZ)_2$] were of sorption ability by high adsorption capacity.

The adsorbent was recovered by 0.10 M HCl and 0.10 M ethylenediamminetetraacetate (EDTA) solution, and the per cent removal remained around 80.7% in the fourth cycle.

The comparison between the performances of SBA-15/DZ adsorbent for simultaneous adsorption of Hg^{2+}, Cu^{2+} and Cd^{2+} ions with various adsorbents is shown in Table 6. As shown, the sum of adsorption capacity for SBA-15/DZ for simultaneous adsorption (87.13 mg g^{-1}) is higher than other simultaneous adsorbents.

4. Conclusions: In this Letter, the mesoporous silica SBA-15/DZ was synthesised by the hydrothermal method to remove heavy metal ions. Interaction [$M(DZ)_2$] complex with mesoporous silica SBA-15 was suitable for simultaneous removal of Hg^{2+}, Cu^{2+} and Cd^{2+} heavy metal ions in aqueous solution and environmental samples, because SBA/[$M(DZ)_2$] have more activated adsorption sites than SBA-15 and DZ singly. This sorbent has high adsorption capacity and selectivity, rapid sorption/desorption kinetic and recovered easily by EDTA and HCl solution. The equilibrium and kinetic studies were investigated for the adsorption process. The isotherm models such as Langmuir, Freundlich and Tempkin were evaluated and the equilibrium data were best described by the Langmuir model. The process kinetics can be successfully fitted to the pseudo-second-order kinetic model.

5. Acknowledgments: The financial support of this Letter by the Iran University of Science and Technology and Iran Nanotechnology Initiative Council is gratefully acknowledged.

6 References

[1] Azimpanah R., Solati Z., Hashemi M.: 'Green synthesis of silver nanoparticles and their applications as a colorimetric probe for determination of Fe^{3+} and Hg^{2+} ions', *IET Nanobiotechnol.*, 2018, **12**, pp. 673–677

[2] Liang C., Feng X., Yu J., *ET AL.*: 'Facile one-step hydrothermal syntheses of graphene oxide–MnO_2 composite and their application in removing heavy metal ions', *Micro Nano Lett.*, 2018, **13**, pp. 1179–1184

[3] Zeeb M., Mirza B., Zare-Dorabei R., *ET AL.*: 'Ionic liquid-based ultrasound-assisted in situ solvent formation microextraction combined with electrothermal atomic absorption spectrometry as a practical method for preconcentration and trace determination of vanadium in water and food samples', *Food Anal. Methods*, 2017, **7**, pp. 1783–1790

[4] Zare-Dorabei R., Dashtian K., Jalalat V.: 'Lanthanum (III) ion determination by a new design optical sensor', *IEEE Sens. J.*, 2015, **15**, pp. 6715–6721

[5] Shenashen M.A., Elshehy E.A., El-Safty S.A., *ET AL.*: 'Visual monitoring and removal of divalent copper, cadmium, and mercury ions from water by using mesoporous cubic Ia3d aluminosilica sensors', *Sep. Purif. Technol.*, 2013, **116**, pp. 73–86

[6] Fernández-Lodeiro J., Nuñez C., Fernández-Lodeiro A., *ET AL.*: 'New-coated fluorescent silver nanoparticles with a fluorescein thiol ester derivative: fluorescent enhancement upon interaction with heavy metal ions', *J. Nanoparticle Res.*, 2014, **16**, pp. 2315–2327

[7] Liu Z., Wang D., Yang S., *ET AL.*: 'Selective recovery of mercury from high mercury-containing smelting wastes using an iodide solution system', *J. Hazard. Mater.*, 2019, **363**, pp. 179–186

[8] Zare-Dorabei R., Rahimi R., Koohi A., *ET AL.*: 'Preparation and characterization of a novel tetrakis(4–hydroxyphenyl) porphyrin–graphene oxide nanocomposite and application in an optical sensor and determination of mercury ions', *RSC Adv.*, 2015, **5**, pp. 93310–93317

[9] Shenashen M.A., El-Safty S.A., Elshehy E.A.: 'Architecture of optical sensor for recognition of multiple toxic metal ions from water', *J. Hazard. Mater.*, 2013, **260**, pp. 833–843

[10] Yang G., Tang L., Lei X., *ET AL.*: 'Cd(II) removal from aqueous solution by adsorption on _*a*-ketoglutaricacid-modified magnetic chitosan', *Appl. Surf. Sci.*, 2014, **292**, pp. 710–716

[11] Awual M.R., Yaita T., El-Safty S.A., *ET AL.*: 'Copper(II) ions capturing from water using ligand modified a new type mesoporous adsorbent', *Chem. Eng. J.*, 2013, **221**, pp. 322–330

[12] Awual M.R., Yaita T., Okamoto Y.: 'A novel ligand based dual conjugate adsorbent for cobalt (II) and copper (II) ions capturing from water', *Sens. Actuators B, Chem.*, 2014, **203**, pp. 71–80

[13] Shirzadmehr A., Afkhami A., Madrakian T.: 'A new nano-composite potentiometric sensor containing an Hg^{2+}-ion imprinted polymer for the trace determination of mercury ions in different matrices', *J. Mol. Liq.*, 2015, **204**, pp. 227–235

doi: 10.1049/mnl.2018.5775

[14] Thinh N.N., Hanh P., Ha L., *ET AL.*: 'Magnetic chitosan nanoparticles for removal of Cr(VI) from aqueous solution', *Mater. Sci. Eng.*, 2013, **33**, pp. 1214–1218
[15] Uygun M., Feyzioglu E., Ozcaliskan E., *ET AL.*: 'New generation ion-imprinted nanocarrier for removal of Cr(VI) from wastewater', *J. Nanoparticle Res.*, 2013, **15**, pp. 1833–1839
[16] Faisal M., Ismail A.A., Harraz F.A., *ET AL.*: 'Mesoporous TiO_2 based optical sensor for highly sensitive and selective detection and preconcentration of Bi(III) ions', *Chem. Eng. J.*, 2014, **243**, pp. 509–516
[17] Wu S., Li F., Xu R., *ET AL.*: 'Synthesis of thiol-functionalized MCM-41 mesoporous silicas and its application in Cu(II), Pb (II), Ag (I) and Cr(III) removal', *J Nanoparticle Res.*, 2010, **12**, pp. 2111–2124
[18] Dashtian K., Zare-Dorabei R.: 'Synthesis and characterization of functionalized mesoprous SBA-15 decorated with Fe_3O_4 nanoparticles for removal of Ce (III) ions from aqueous solution: 'ICP–OES detection and central composite design optimization', *J. Colloid Interface Sci.*, 2017, **494**, pp. 114–123
[19] Zhang M., Wang W., Zhu Z., *ET AL.*: 'One-step synthesis of amino-functionalised magnetic mesoporous silica and synergistic adsorption kinetics of tetracycline and copper', *Micro Nano Lett.*, 2018, **13**, pp. 1219–1223
[20] Zare-Dorabei R., Jalalat V., Tadjarodi A.: 'Central composite design optimization of Ce(III) ion removal from aqueous solution using modified SBA-15 mesoporous silica', *New J. Chem.*, 2016, **40**, pp. 5128–5134
[21] Kalantari K., Ahmad M.B., Fard Masoumi H.R., *ET AL.*: 'Rapid adsorption of heavy metals by Fe_3O_4/talc nanocomposite and optimization study using response surface methodology', *J. Mol. Sci.*, 2014, **15**, pp. 12913–12927
[22] Nourozi S., Zare-Dorabei R.: 'Highly efficient ultrasonic-assisted removal of methylene blue from aqueous media by magnetic mesoporous silica; experimental design methodology, kinetic and equilibrium studies', *Desalination Water Treat.*, 2017, **85**, pp. 184–196
[23] Dashtian K., Zare-Dorabei R., Jafarinia R., *ET AL.*: 'Application of central composite design for optimization of preconcentration and determination of La (III) ion in water samples using the SBA-15–HESI and SBA-15–HESI-Fe_3O_4–NPs sorbents', *J. Environ. Chem. Eng.*, 2017, **5**, pp. 5233–5240
[24] Saghanejhad Tehrani M., Zare-Dorabei R.: 'Competitive removal of hazardous dyes from aqueous solution by MIL-68(Al): derivative spectrophotometric method and response surface methodology approach', *Spectrochim. Acta A*, 2016, **160**, pp. 8–18
[25] Chen F., Yuan Y., Chen C., *ET AL.*: 'Investigation of colloidal biogenic sulfur flocculation: 'optimization using response surface analysis', *J. Environ. Sci.*, 2016, **42**, pp. 227–235
[26] Saghanejhad Tehrani M., Zare-Dorabei R.: 'Highly efficient simultaneous ultrasonic-assisted adsorption of methylene blue and rhodamine B onto metal organic framework MIL-68(Al): central composite design optimization', *RSC Adv.*, 2016, **6**, pp. 27416–27425
[27] Jamshidi M., Ghaedi M., Dashtian K., *ET AL.*: 'Highly efficient simultaneous ultrasonic assisted adsorption of brilliant green and eosin B onto ZnS nanoparticles loaded activated carbon: artificial neural network modeling and central composite design optimization', *Spectrochim. Acta A*, 2016, **153**, pp. 257–267
[28] Kurko S.V., Matović L.L.: 'Simultaneous removal of Pb^{2+}, Cu^{2+}, Zn^{2+} and Cd^{2+} from highly acidic solutions using mechanochemically synthesized montmorillonite–kaolinite/TiO_2 composite', *Appl. Clay Sci.*, 2015, **103**, pp. 20–27
[29] Arcibar Orozco J.A., Rangel Mendez J.R., Diaz Flores P.E.: 'Simultaneous adsorption of Pb (II)-Cd (II), Pb (II)-phenol, and Cd (II)-phenol by activated carbon cloth in aqueous solution', *Water Air Soil Pollut.*, 2015, **226**, pp. 1–10
[30] Perez-Quintanilla D., Del Hierro I., Fajardo M., *ET AL.*: 'Preparation of 2-mercaptobenzothiazole-derivatized mesoporous silica and removal of Hg(II) from aqueous solution', *J. Environ. Monit.*, 2016, **8**, pp. 214–222
[31] Soares I.V., Vieira E.G., Dias Filho N.L., *ET AL.*: 'Study of adsorption and preconcentration by using a new silica organomodified with [3–(2, 2′-dipyridylamine) propyl] groups', *J. Sep. Sci.*, 2013, **36**, pp. 817–825
[32] Hur J., Shin J., Yoo J., *ET AL.*: 'Competitive adsorption of metals onto magnetic graphene oxide: comparison with other carbonaceous adsorbents', *Sci. World J.*, 2015, **2015**, pp. 1–11, doi: 10.1155/2015/836287
[33] Hadavifar M., Bahramifar N., Younesi H., *ET AL.*: 'Adsorption of mercury ions from synthetic and real wastewater aqueous solution by functionalized multi-walled carbon nanotube with both amino and thiolated groups', *Chem. Eng. J.*, 2014, **237**, pp. 217–228
[34] Yuan Y., Zhang G., Li Y., *ET AL.*: 'Poly (amidoamine) modified graphene oxide as an efficient adsorbent for heavy metal ions', *Polym. Chem.*, 2013, **4**, pp. 2164–2167